https://doi.org/10.48048/tis.2024.7311

Synthesis and Characterization of Sorbitol Membraneless Alkaline Fuel Cell Catalysts for Cathode and Anode, Utilizing AgV_2O_5/C, $AgMnO_2/C$, and $PdCeO_2/C$ Catalysts

Chakkrapong Chaiburi[*] and Pintira Chayboonchoo

Department of Chemistry, Faculty of Science, Thaksin University, Phatthalung Campus, Phatthalung 93210, Thailand

([*]Corresponding author's e-mail: chakkrapong@tsu.ac.th)

Received: 12 July 2023, Revised: 8 September 2023, Accepted: 28 September 2023, Published: 20 January 2024

Abstract

This study aimed to develop sorbitol fuel cell catalysts for cathode and anode fuels by synthesizing AgV_2O_5/C, $AgMnO_2/C$, and $PdCeO_2/C$ catalysts. The physical characteristics of the catalysts were analyzed using SEM and EDS. The results showed that the prepared catalysts were small, lumpy, and densely clustered on the carbon surface with small particles. The electrochemical characteristics of the oxidation of alkaline fuels using sorbitol as fuel were investigated by assessing sorbitol concentration ratios of 0.1, 0.2, 0.3, 0.4 and 0.5 per 0.1 M alkaline KOH solution through cyclic voltammetry. The $PdCeO_2/C$ catalyst at a concentration of 0.1 M sorbitol solution exhibits the highest potential difference at the potential range of -0.5 to 0.5 V, resulting in a maximum current density of 0.2 mA/cm^2. The AgV_2O_5/C and $AgMnO_2/C$ catalysts were tested in the reduction reaction, and the concentration ratios of sorbitol solution per 0.1 M alkaline KOH solution varied from 0.1 to 0.5 M. The results demonstrated a decrease in activity in the catalyst reduction reaction as the sorbitol solution concentration increased, indicating a potential correlation with enhanced oxidation resistance.

Keywords: Alkaline fuel cell, Catalyst, Sorbitol, Oxidation reaction, Reduction reaction, Fuel cell, Cathode, Anode

Introduction

Due to a range of environmental concerns, such as global warming, depletion of fossil fuel resources, and the negative impact of pollutants, the use of renewable energy sources for electricity generation has been increasing. The use of fuel cells has become increasingly popular due to their ability to operate on hydrogen gas, making them a clean and highly efficient source of energy. Fuel cells are considered a promising technology for sustainable development because they use hydrogen, a clean energy source that only produces water, heat, and electricity as byproducts [1].

Currently, there are various developments in fuel cell technology that offer different levels of efficiency, ranging from low-cost and low-efficiency systems to high-performance and high-efficiency systems. Among them, alkaline fuel cells have gained wide attention due to their ability to accelerate the fuel cell reaction faster under alkaline conditions than in acidic conditions. Moreover, non-platinum catalyze have shown excellent performance in such an environment [2]. Research has been conducted to investigate catalysts that can be used as substitutes for many platinum metals. Palladium metal has been found to be a suitable substitute for platinum metal [3]. Platinum metal as the cathode and anode catalysts are frequently catalysts used in studies to catalysts the reduction reactions of oxidants. According to studies on platinum-based catalysts, such catalysts provide good fuel cell performance. However, due to the relatively high cost of platinum metal, commercial investments are not considered. In order to tackle these issues, the development of cathode catalysts with other metals has been increasingly studied. This research delved into the electrochemical properties of carbon-supported silver/metal oxide-based catalysts, specifically AgVxOy/C and AgMnxOy/C. The aim was to assess their potential as cathode electrodes for reducing sugar as fuel in alkaline fuel cells operating without an exchange membrane. The physical attributes of these catalysts underwent scrutiny via scanning electron microscopy, while their elemental composition was ascertained through energy dispersive x-ray spectroscopy. The electrochemical features of the catalytic reduction reaction were analyzed using cyclic voltammetry [4]. Silver nanoparticles supported on carbon (Ag:NPs/C) were fabricated through a gamma irradiation-induced reduction technique, employing either poly(vinyl alcohol) or a combination of poly(vinyl alcohol) and chitosan

polymers as stabilizers. The resulting specimens underwent characterization using transmission electron microscopy and X-ray diffractometry. Subsequently, the electrocatalytic potential of Ag:NPs/C was examined for both the oxygen reduction reaction (ORR) and the borohydride oxidation reaction (BOR) using the rotating disc and rotating ring disc methods. These investigations aimed to assess their suitability for potential applications in alkaline fuel cells [5]. Ag-MnOx/C composites were synthesized using $AgNO_3$ and $KMnO_4$ as precursors, with Vulcan XC-72 serving as the support material. The physical characteristics of these composites were thoroughly examined through X-ray diffraction (XRD), X-ray photoelectron spectroscopy (XPS), and transmission electron microscopy (TEM). Their performance and stability in catalyzing the oxygen reduction reaction (ORR) in alkaline environments were evaluated using electrochemical techniques. The results reveal that in the fresh sample, the primary components, MnO_2, and Ag_2O, transform into Mn_3O_4 and Ag(0), respectively, after heat treatment in an N_2 atmosphere at 300 °C, resulting in the Ag-MnOx/C-300 composite. Notably, the Ag-MnOx/C-300 sample demonstrates the highest ORR activity. When applied as the air electrode in a zinc-air battery, it achieves a remarkable maximum power density of 130 MW cm^{-2}. This performance surpasses that of cathode catalysts based on Pd/C and Pt/C, underscoring the potential of the Ag-MnOx/C-300 composite as a promising catalyst for air electrodes [6]. The PdCeOx/C catalyst was synthesized and examined as the anodic catalyst for formic acid electrooxidation. Its characteristics, composition, and electrocatalytic performance were scrutinized using transmission electron microscopy, energy-dispersive X-ray analysis, X-ray diffraction, X-ray photoelectron spectroscopy, linear sweep voltammetry, and chronoamperometry, respectively. The Pd nanoparticles in the PdCeOx/C catalyst displayed an average size of approximately 3.4 nm and exhibited a narrow size distribution. Electrochemical assessments revealed the outstanding catalytic activity and stability of the PdCeOx/C catalyst. Notably, the peak current for formic acid oxidation on the PdCeOx/C catalyst was approximately 1.67 times that of the Pd/C catalyst, and the stable current at 3,600 s was approximately 7 times that of the Pd/C catalyst. This enhancement is attributed to the larger electrochemically active surface area (ESA), electronic effects, and the presence of more oxygen-containing species facilitated by the CeOx. Consequently, this catalyst holds promise for applications in direct formic acid fuel cells [7]. Sorbitol represents a promising and cost-effective fuel derived from renewable biomass sources. Surprisingly, the electro-oxidation reaction of sorbitol (SOR), despite its sustainable nature, has received limited attention. Existing studies have predominantly utilized bulky or nanoparticulate Pt-based materials, which exhibit subpar activity. This study introduces an eco-friendly approach for synthesizing nanomaterials, including Au/C, Pd/C, and Au–Pd/C, as alternative electrocatalysts to Pt, with a focus on assessing their efficacy in catalyzing sorbitol electro-oxidation. The electrocatalytic assessment of SOR at room temperature revealed that Pd/C demonstrated an almost 3.5-fold increase in current density compared to commercial Pt/C. Au/C exhibited comparable activity to Pt/C, whereas Au–Pd/C displayed a 2-fold greater current density than Pt/C at a lower overpotential (60 mV). The investigation of these materials also extended to evaluating their performance in the electro-oxidation of the primary sorbitol byproducts, namely glucose and gluconic acid. This comprehensive analysis indicated that the exceptional current density exhibited by Pd/C in sorbitol oxidation can be attributed to a higher electron transfer per sorbitol molecule [8]. The impact of the secondary metal in AuM (M: Ag, Pd and Pt) materials on the electro-oxidation of sorbitol (SOR) in an alkaline environment was examined. The resulting nanoparticles exhibited a similar average particle size of approximately 7 nm. The gold content varied from 53 to 77 atomic %, and the loading of Vulcan carbon support was about 80 ± 5 wt%. Cyclic voltammograms conducted using 0.1 M sorbitol in 0.3 M KOH revealed that AuPt/C exhibited the lowest onset potential (−0.36 V vs. NHE), notably 120 mV lower than that of the reference material, Au/C. Additionally, the AuPd/C catalyst demonstrated the highest current density (43.65 ($mA.mg_{AuPd}^{-1}$)) at a consistent potential of 0.14 V vs. NHE. In conclusion, this study concludes that materials containing AuPd and Pd show promising potential for catalyzing sorbitol oxidation in an alkaline medium [9]. Sorbitol, a readily available and functionalized polyalcohol with widespread industrial applications, holds significant promise for fuel cell usage. However, more research needs to be conducted on its electrochemical oxidation. This study involves the synthesis of monometallic Au, Pt, and PtAu nanomaterials with varying compositions, spanning from Pt-rich (e.g., $Pt_{85}Au_{15}$) to Au-rich ($Pt_{10}Au_{90}$). Notably, the PtAu nanomaterials demonstrated an augmentation in current density with increasing concentrations of KOH and sorbitol. Notably, among these materials, $Pt_{40}Au_{60}$/C emerged as the most potent electrocatalyst, exhibiting a current density of 40 mA mg^{-1} at 0.1 M sorbitol in 2 M KOH, along with an onset potential of −0.50 V vs. NHE. This onset potential value was more negative than the typical reports for other polyols, such as glycerol and ethylene glycol. The impressive electrocatalytic performance of $Pt_{40}Au_{60}$/C was attributed to changes in electron density that facilitated heightened electron transfer, leading to shorter-chain [10]. The objective of this study was to assess the viability of Pd/C, Ag/C, AgVxOy/C, VxOy/C, and W/C catalysts as glycerol-tolerant materials, with the aim of potential utilization

in the cathodes of alkaline glycerol fuel cells. A thorough analysis of the surface characteristics and metal distribution across these catalysts consistently demonstrated uniform features and even metal dispersion on their respective support materials. In the absence of glycerol, Pd/C, Ag/C, and AgVxOy/C catalysts displayed superior catalytic efficiency in reduction reactions compared to their W/C counterparts. Upon the introduction of glycerol, the evaluation of catalytic reduction reactions indicated that both Ag/C and AgVxOy/C catalysts exhibited glycerol tolerance, as they did not undergo oxidation reactions. Consequently, these catalysts hold significant promise for potential integration into the cathodes of alkaline fuel cells [11].

This work studies the electrooxidation of sorbitol fuel in alkaline (KOH) solutions, which use AgV_2O_5/C, $AgMnO_2$/C, and $PdCeO_2$/C as an electrical catalyst. This investigation was to examine the structural properties of the catalyst and assess its electrochemical efficiency in promoting the oxidation of sorbitol in fuel solutions. There are several reasons for using sorbitol as a fuel in alkaline fuel cells.

Renewable and sustainable

Sorbitol can be derived from renewable sources such as corn or other biomass. This makes it an environmentally friendly and sustainable fuel option, reducing dependence on fossil fuels.

High hydrogen content

Sorbitol is a polyalcohol, and it contains a relatively high percentage of hydrogen by weight. Hydrogen is a key component in fuel cells, as it reacts with oxygen to produce electricity.

Low toxicity

Sorbitol is relatively nontoxic, which is important for safety considerations in fuel cell applications. It poses fewer health and environmental risks compared to some other potential fuels.

Ease of handling

Sorbitol is a liquid at room temperature, which makes it easier to handle and transport compared to gaseous fuels like hydrogen. This simplifies the fuel delivery system.

Compatibility with alkaline conditions

Alkaline fuel cells operate in an alkaline environment, and sorbitol is stable under these conditions. It can be used directly without the need for complex fuel reforming processes.

Reduced CO_2 emissions

When sorbitol is used as a fuel in alkaline fuel cells, the primary byproduct is water, and the process generally produces lower carbon dioxide (CO_2) emissions compared to burning fossil fuels.

Overall, these factors contribute to sorbitol's potential as a promising fuel option for alkaline fuel cells, especially in applications where sustainability, safety, and ease of handling are important considerations.

Materials and methods

Catalyst synthesis

Catalyst of cathode AgVxOy/C and AgMnxOy/C

AgVxOy/C

Step 1 Take silver nitrate ($AgNO_3$) 0.157 g and vanadium pentoxide (V_2O_5) 0.357 g. Dissolve in 50 mL of deionized water and then stir with magnetic stirrers for 2 h. Then adjust the pH to 9 - 11 by using a NaOH 2 molar solution, then add 1.5 g of sodium borohydride ($NaBH_4$), stirring with magnetic Stirrers for 30 min. The sediment is then filtered and washed with deionized water several times, and the sediment is dried at 80 °C for 24 h to form silver vanadium oxide compounds.

Step 2 VulcanXC–72R carbon 0.80 g is added to the silver vanadium oxide compound. Then add 50 mL of deionized water. The prepared solution is then mixed with magnetic stirrers for 2 h, after which the sediment is filtered and washed with magnetic stirrers several times. The sediment is then dried at 80 °C for 24 h to form silver vanadium oxide compounds on carbon.

AgMnxOy/C

Step 1 Take silver nitrate ($AgNO_3$) 0.157 g and manganese (II) oxide (MnO_2) 0.10 g. Dissolve in 50 mL of deionized water and then stir with magnetic stirrers for 2 h. The pH is then adjusted to 9 - 11 using a NaOH 2 molar solution. Sodium borohydride ($NaBH_4$) 1.5 g and Vulcan XC–72R carbon 0.8 g, then

stirred with magnetic stirrers for 2 h. The sediment is then filtered and washed with deionized water several times, and the sediment is dried at 80 °C for 24 h to form silver manganese oxide on carbon.

Catalyst of anode PdCexOy/C

PdCexOy/C

Step 1 The cerium oxide compound (CeOx) 0.2 g. Dissolve in 50 mL of deionized water, then stir with magnetic stirrers for 30 min. Next, the pH is adjusted to 9 - 11 by using a NaOH 2 molar solution and of vulcan XC–72R Carbon 0.8 g, then stirred with magnetic stirrers for 24 h. The sediment is then filtered and washed with deionized water several times, and the sediment is dried at 80 °C for 24 h to form cerium oxide on carbon.

Step 2 Palladium (II) chloride ($PdCl_2$) 0.2 g and cerium oxide are added. Then deionized water 50 mL was added, and the solution was mixed with magnetic stirrers for 2 h. Sodium borohydride ($NaBH_4$) 1.5 g is then added, after which the sediment is filtered and washed with deionized water several times. The sediment is dried at 80 °C for 24 h to form palladium cerium oxide on carbon.

Catalyst lnk

Prepare a solution of 0.009 g of catalyst concentration in 5 mL of solution by weighing 0.009 g of the catalyst. Then add to a mixture of 3.5 mL of isopropanol solution and 1.5 mL of DI water, after which the substances are dissolved together by the ultrasonic method.

Preparation of the working electrode

Preparation of the working electrodes starts by wiping the glassy carbon on the working electrode with ethanol solution 1 - 2 times. Once the ethanol solution is completely evaporated, a drop of 1.5 microliter of nafion solution is added. Set aside for 3 min. After that, 5 µl of the catalyst solution is added and left for 24 h. The working electrode containing the catalyst can then be obtained.

Physical characterization of the catalyst

The physical characteristics of the electrocatalyst samples were studied using scanning electron microscopy (FE-SEM, FEI brand, model Quanta 450 FEG), and the elemental composition was analyzed using energy-dispersive X-ray spectroscopy (EDS Oxford Instruments X-Max 50).

SEM sample preparation

Before conducting SEM characterization, it is essential to ensure that samples are completely dried to prevent any outgassing caused by organic contamination or moisture.

Sample mounting

Typically, samples are affixed to holders or stubs using double-sided conductive tape. It's crucial to utilize the vacuum-compatible carbon and copper tapes provided by the SEM laboratory.

Powder samples

Preparing powder materials for SEM can be challenging due to difficulties in mounting. Special care is required to prevent samples from detaching and scattering within the vacuum environment or under the electron beam. For small quantities of powder, a method involves evenly spreading the powder onto a clean substrate. After thorough drying, the individual powder particles should be well-dispersed across the substrate surface.

Electrochemical characterization of catalyst

The electrochemical characteristics of the electrocatalyst samples were studied by cyclic voltammetry (CV). The parameters were set to have a voltage range from −1.2 to 1.2 V, a rough scan rate of 100 mV/s, and a fine scan rate of 10 mV/s.

This research studied the electrochemical characteristics of sorbitol solution for use as a fuel for the cathode (positive electrode) and anode (negative electrode) of alkaline fuel cells based on silver vanadium alloy, silver manganese oxide, and palladium cerium oxide on carbon. The physical characteristics and potential of silver vanadium alloy electrocatalysts were also studied, silver manganese oxide and palladium cerium oxide on carbon support. The scope of this study was divided into 2 parts. The first studied the physical characterization of silver vanadium alloy electrocatalysts, namely silver, manganese oxide, and palladium cerium oxide, on carbon support with scanning electron microscopy and elemental analysis by the energy elemental analysis technique. The second part investigated the electrochemical characterization

of silver vanadium alloy electrocatalysts, silver, manganese oxides, and palladium cerium oxides on carbon in the oxidation of sorbitol fuel in an alkaline solution (KOH) by the cyclic voltammetry technique.

Results and discussion

Physical characterization of the catalyst

The initial stage of this research involves examining the physical properties of 3 different electrocatalysts on carbon substrates. Specifically, silver vanadium catalysts, silver manganese oxide, and palladium cerium oxide on carbon carriers will be studied using scanning electron microscopy (SEM) and energy-dispersive X-ray spectroscopy (EDS) techniques.

Scanning electron microscopy (SEM) techniques

The AgVxOy/C catalyst appears as agglomerated clusters on the carbon surface, featuring small particles that are densely packed (**Figure 1**). Morphological assessments of the nanocomposites were conducted at 2 levels of magnification to assess the overall architectures of the nanocomposites and the dispersion of Ag and V nanoparticles within the supporting materials (**Figure 4**).

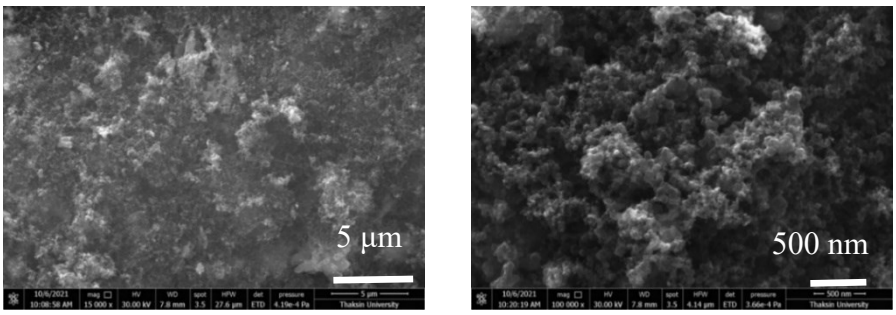

Figure 1 Scanning electron microscopy micrograph that illustrates the physical characteristics of the AgVxOy/C catalyst.

The AgMnxOy/C catalysts exhibit substantial, closely packed clusters containing dispersed small particles on the carbon surface, as depicted in **Figure 2**. Morphological assessments of the nanocomposites were conducted at 2 magnification levels to assess both the overall architectures of the nanocomposites and the distribution of Ag and Mn nanoparticles within the supporting materials (**Figure5**).

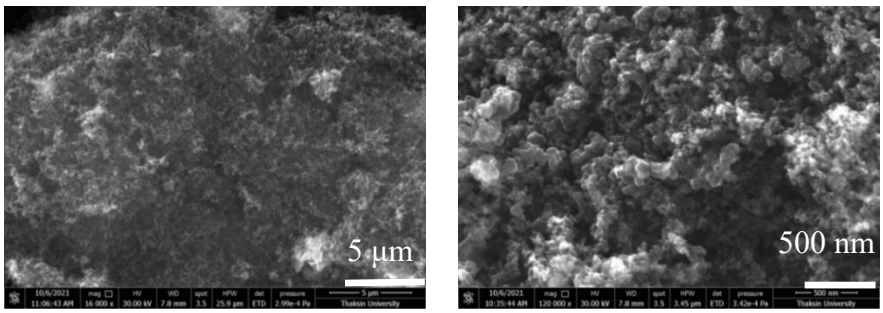

Figure 2 Scanning electron microscopy micrograph that illustrates the physical characteristics of the AgMnxOy/C catalyst.

As illustrated in **Figure 3**, the PdCexOy/C catalyst forms dense clusters on the carbon surface, accompanied by a notable concentration of small, irregular particles. Morphological analysis of the nanocomposites was conducted at 2 magnification levels to assess the overall architectures of the nanocomposites and the dispersion patterns of Pd and Ce nanoparticles within the supporting materials (**Figure 6**).

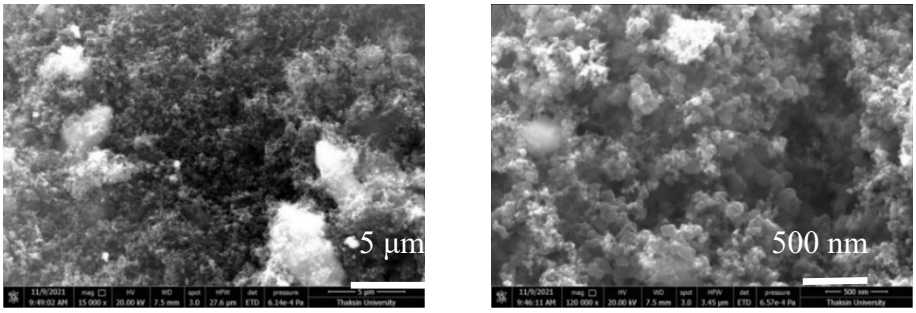

Figure 3 Scanning electron microscopy micrograph that illustrates the physical characterisation of the PdCexOy/C catalyst.

The catalysts display densely packed clusters alongside dispersed small particles on the carbon surface. The catalyst's physical characteristics were explored using the SEM technique. As indicated in **Table 1**, distinct preparation methods yielded varying properties due to the insufficient repulsion of charges to induce separation. The aggregation of metal catalysts on the carbon support will influence the electrochemical reaction area, a topic that will be investigated concerning the electrocatalyst's potential.

Energy-dispersive x-ray spectroscopy (EDS) technique

The AgVxOy/C catalyst measured EDS. Elemental compositions were C 87.25 wt%, Ag 1.7 wt% and V 1.99 wt% (**Figure 4**).

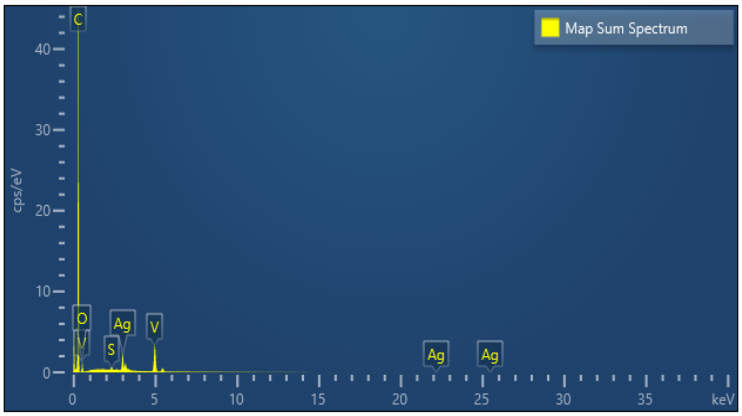

Figure 4 The elemental composition of AgVxOy/C.

The AgMnxOy/C catalyst measured EDS. The elemental composition was C 93.54 wt%, Ag 0.67 wt%, and Mn 0.89 wt% (**Figure 5**).

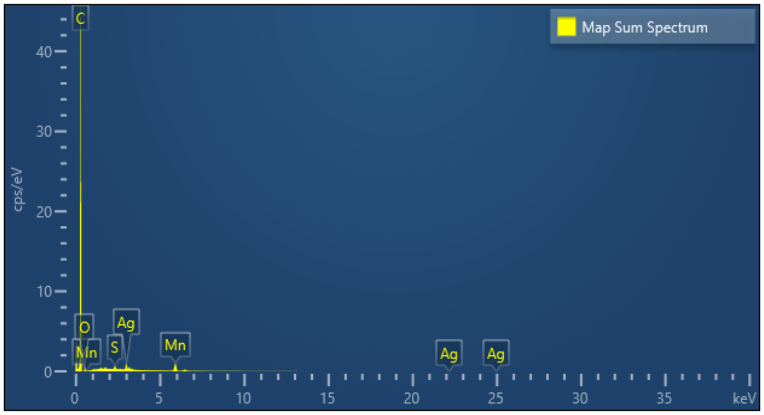

Figure 5 The composition of elemental AgMnxOy/C.

The PdCexOy/C catalyst measured EDS, the elemental composition of C 92.01 wt%, Pd 3.19 wt%, and Ce 4.59 wt% (**Figure 6**).

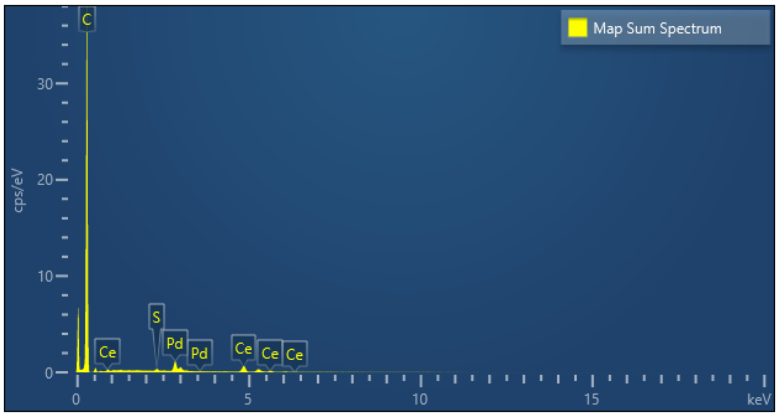

Figure 6 The composition of the element PdCexOy/C.

The EDS technique allows us to discern distinct elemental components within the catalyst, as illustrated in **Figures 4 - 6**. These variations in elemental values are likely influenced by the catalyst's distribution across the carbon surface. Discuss how the detected X-rays are used to identify the elements present in the sample. Each element has characteristic X-ray emissions at specific energy levels. By analyzing the energy and intensity of these X-rays, the EDS system can determine which elements are present in the sample. Highlight that the output of an EDS analysis is a spectrum showing peaks at specific energy levels. Each peak corresponds to an element's characteristic X-ray emission. The intensity of the peaks represents the relative abundance of each element.

XRD Structural analysis

Wide-angle XRD corroborated the development of crystalline $AgMnO_2$, as illustrated in **Figure 7**. The Ag's XRD pattern revealed peaks corresponding to (111), (200), (220), and (311), demonstrating its crystalline nature with a face-centered cubic structure JCPDS. NO: 01-073-6976. The MnO_2 XRD pattern indicated peaks for (110), (101), and (211), confirming the crystalline nature with a tetragonal structure (pyrolusite) JCPDS. NO: 01-071-4824.

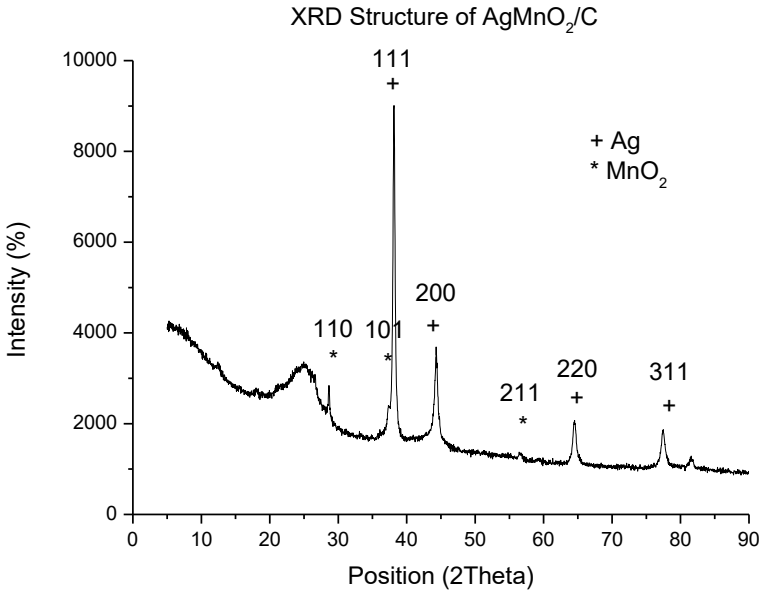

Figure 7 Diffractrograms of the $AgMnO_2$/C catalyst.

Wide-angle X-ray diffraction (XRD) analysis confirmed the production of crystalline silver (Ag), as depicted in **Figure 8**. The XRD pattern of Ag exhibited distinct peaks corresponding to the crystallographic planes (111), (200), (220), (222), and (311), which provided evidence of its higher order crystalline nature with a face-centered cubic structure. These results were consistent with the JCPDS reference code: 01-073-6976, which corresponds to the face-centered cubic structural phase of silver. Similarly, the XRD pattern of V_2O_5 revealed peaks corresponding to the crystallographic planes (001), (110), (101), (200), (301), (310), (411), (600), (601), (421), (403), and (503), indicating the crystalline nature of V_2O_5 with an orthorhombic structure. The Joint Committee on Powder Diffraction Standards (JCPDS) reference code 00-041-1426 supports these findings.

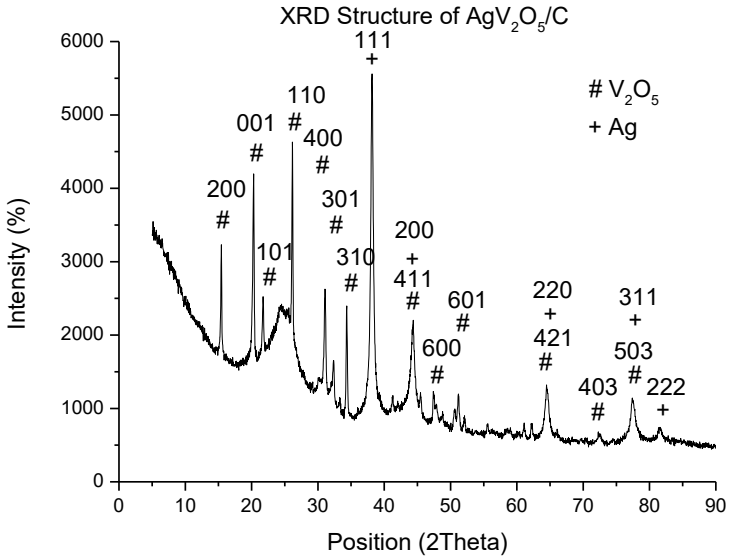

Figure 8 Diffractrograms of the AgV_2O_5/C catalyst.

The presence of crystalline palladium (Pd) was confirmed through wide-angle X-ray diffraction (XRD) analysis, as depicted in **Figure 9**. The XRD pattern of Pd displayed distinct peaks corresponding to the crystallographic planes (111) and (220), which provided evidence of its crystalline nature with a cubic structure. This observation aligns with the JCPDS reference code: 01-088-2335, which corresponds to the cubic structural phase of Pd. Similarly, the XRD pattern of CeO_2 revealed peaks corresponding to the crystallographic planes (111), (200), (220), (222), (311), (331), (400), (420), and (422), indicating the crystalline nature of CeO_2 with a cubic structure. These findings are consistent with the JCPDS reference code 01-071-4807.

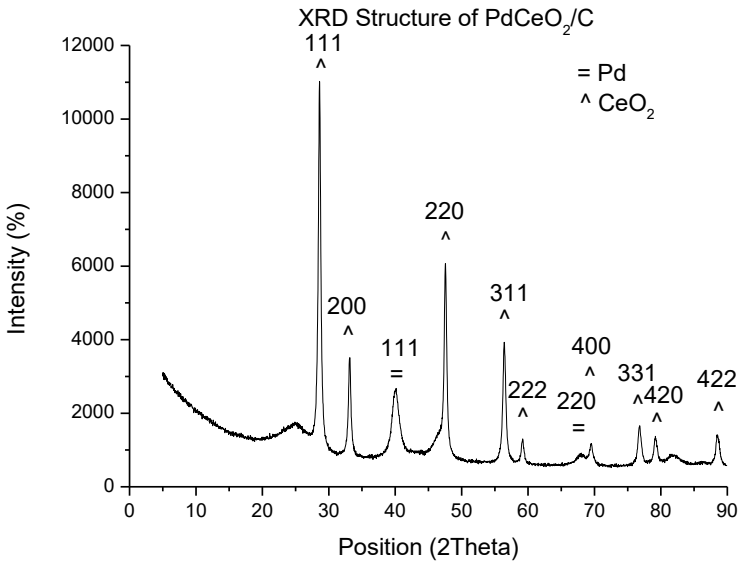

Figure 9 Diffractograms of the $PdCeO_2$/C catalyst.

Electrochemical characterization of the electrocatalysts

The second part of this research studies the influence of 3 types of electrocatalysts on carbon support materials, namely silver vanadium catalyst, silver manganese oxide, and palladium cerium oxide on carbon carriers on the electrochemical characteristics of sorbitol fuel oxidation of 0.1 to 0.5 in 0.1 M KOH solution by cyclic voltammetry.

Catalyst for cathode electrodes (Cathodic)

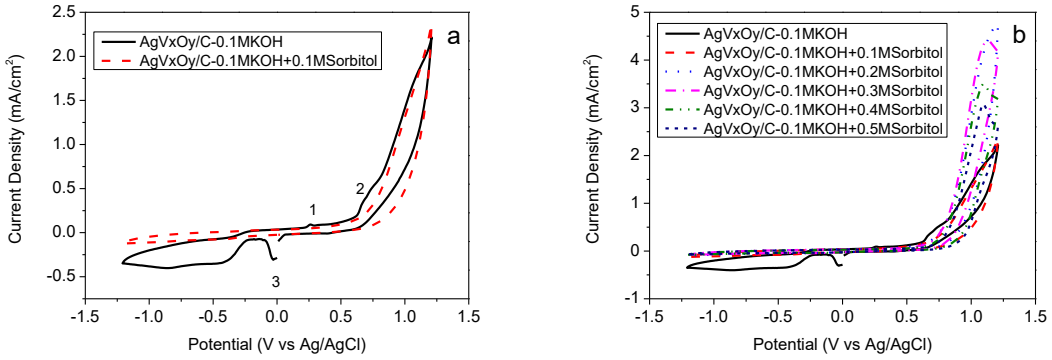

Figure 10 Cyclic voltammogram of AgV_2O_5/C catalyst in 0.1 M KOH solution doped with 0.0 to 0.1 M sorbitol at a scan rate of 0.01 V/s (a). Cyclic voltammogram of AgV_2O_5/C catalyst in 0.1 M KOH solution doped with 0.0 to 0.5 M sorbitol at a scan rate of 0.01 V/s (b).

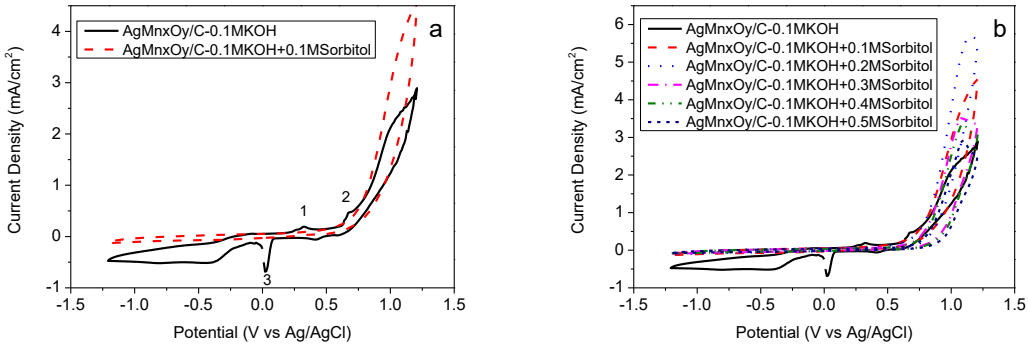

Figure 11 Cyclic voltammogram of $AgMnO_2$/C catalyst in 0.1 M KOH solution doped with 0.0 to 0.1 M sorbitol at a scan rate of 0.01 V/s (a). Cyclic voltammogram of $AgMnO_2$/C catalyst in 0.1 M KOH solution doped with 0.0 to 0.5 M sorbitol at a scan rate of 0.01 V/s (b).

The AgV_2O_5/C and $AgMnO_2$/C catalysts were tested in a 0.1 M KOH solution doped with sorbitol at concentrations of 0.0 - 0.5 M. The doping with sorbitol solution affected the reduction reaction, as shown in **Figures 10(b)** and **11(b)**. Cyclic voltammograms were recorded from the AgV_2O_5/C and $AgMnO_2$/C catalysts in a 0.1 M KOH solution, both with and without sorbitol doping at concentrations of 0.1, 0.2, 0.3, 0.4, and 0.5 M. The AgV_2O_5/C and $AgMnO_2$/C catalysts (**Figures 10(a)** and **11(a)**) showed 2 oxidation states. At 0.25 V, the formation of a monolayer of AgOH and Ag(I) [12] occurred, while electron adsorption of AgO^- and the formation of the inner hydrous oxide layer occurred at 0.25 to 0.43 V, as shown in position 1. In position 2, a potential of 0.57 to 0.75 V signifies the recovery of the Ag catalyst and the formation of an outer oxide layer for further reaction in the next scanning cycle. Between 0.57 and 0.75 V, the Ag catalyst was electrically recovered, and an outer oxide layer was formed to react in the next scan cycle [12]. The AgV_2O_5/C and $AgMnO_2$/C catalysts are shown in **Figures 10(a)** and **11(a)**, respectively. Scanning of the anodic current region revealed a potential range of 0.75 to 1.10 V associated with the recovery of the Ag catalyst and the development of an outer oxide layer. Position 3 shows the electrical potential in the range of −0.10 to 0.05 V. Silver oxide is continuously formed from the anodic current range [12].

In **Figure 11(a)**, the reduction reaction of the MnO_2 component in the $AgMnO_2$/C catalyst is depicted. The electric potential range from −1.20 to −0.50 V corresponds to the recovery of the MnO_2 catalyst for further scanning cycles, as shown in Eq. (3). This range overlaps with the −0.50 to −0.15 V, which corresponds to the reduction of MnOOH to $MnOOH^-$ (as given in Eq. (2)).

Eqs. (1) - (4) [13] represents the reaction equation of manganese metal;

$$2MnO_2 + 2H_2O + 2e^- \rightarrow 2MnOOH + 2OH^- \quad (1)$$

$$2MnOOH + O_2 \rightarrow 2(MnOOHO^-) \quad (2)$$

$$2(MnOOHO^-) + 2e^- \rightarrow 2MnO_2 + 2OH^- \quad (3)$$

$$\text{Net equation: } O_2 + 2H_2O + 4e^- \rightarrow 4OH^- \quad (4)$$

Figure 10(a) shows the reduction reaction of the V_2O_5 component in the AgV_2O_5/C catalyst. The electric potential range from −1.20 to −0.50 V corresponds to the recovery of the V_2O_5 catalyst for further scanning cycles, as demonstrated in Eq. (8). The presence of metal oxides (V_2O_5) contributes to an improved reduction reaction of the catalyst at lower voltage ranges.

The vanadium-metal reaction represents an Eqs. (5) - (9). [14];

$$2V^VO + 4H^+ + 4e^- \rightarrow 2V^{III} + 2H_2O \quad (5)$$

$$V^{III} + O_2 \rightarrow O_2V \quad (6)$$

$$O_2V + V^{III} \rightarrow [VOOV] \quad (7)$$

$$[VOOV] \rightarrow 2V^{V}O \quad (8)$$

$$\text{Net equation: } O_2 + 4H^+ + 4e^- \rightarrow 2H_2O \quad (9)$$

The AgV_2O_5/C and $AgMnO_2$/C catalyst, when tested at a potential difference of −0.25 to −1.20 V, exhibited reduced reduction reaction compared to the reaction without the sorbitol solution. This can be attributed to the adsorption of the sorbitol solution at the active site of the catalyst, which led to a decrease in current density at the reduction sites. The process of sorbitol solution adsorption at the catalyst's active site was found to be similar to the reaction observed with a sorbitol-adsorbed solution [15].

In **Figures 10** and **11**, peak position one was observed when the catalyst was doped with sorbitol solutions at concentrations of 0.1, 0.2, 0.3, 0.4, and 0.5 M. This is likely due to the sorbitol solution being adsorbed at the catalyst's active site, which could potentially block the oxidation of the alcohol functional groups by hydrocarbons. As the concentration of the sorbitol solution was increased, it is possible that the oxidation of the alcohol functional groups was further blocked.

Eq. (10) and **Figures 10** and **11** demonstrate that the oxygen evolution reaction (OER) decreased as the concentration of sorbitol solution increased at a potential difference ranging from 0.50 to 1.20 V [16].

$$4OH^- \rightarrow O_2 + 4H_2O + 4e^- \quad (10)$$

The AgV_2O_5/C and $AgMnO_2$/C catalysts are cathode-side catalysts, which require reduction reactions. As such, the catalysts must be resistant to oxidation at the cathode. When doped with sorbitol solution at a concentration of 0.1 - 0.5 M, the reduction reaction decreased, making the catalyst resistant to oxidation.

Catalyst for anode (Anodic)

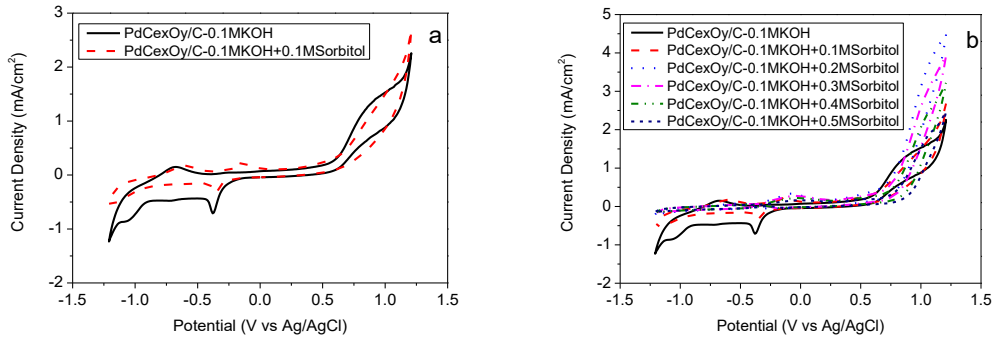

Figure 12 Cyclic voltammograms of the catalyst of $PdCeO_2$/C in 0.1 M KOH solution doped with 0.0 to 0.1 M sorbitol at a scan rate of 0.01 V/s (a). Cyclic voltammograms of the catalyst of $PdCeO_2$/C in 0.1 M KOH solution doped with 0.0 to 0.5 M sorbitol at a scan rate of 0.01 V/s (b).

The redox process of the catalyst was analyzed as a factor affecting the electrochemical characterization, using cyclic voltammetry [17]. The electrochemical characterization technique was used to determine the mechanism of the Pd catalyst's electrochemical reaction at the anode under alkaline conditions. During the forward scan, an oxidation reaction was observed at a potential difference of −1.2 to −0.5 V vs. Ag/AgCl, which involved hydrogen uptake and adsorption on the catalyst surface (as shown in **Figure 12(a)** and represented by Eq. (11)).

$$Pd{-}H_{abs/ads} + OH^- \rightarrow Pd - H_2O + e^- \quad (11)$$

At the potential range of −0.5 to 0.5 V vs. Ag/AgCl, hydroxide ions (OH^-) adsorb onto the Pd catalyst surface, initiating the reaction represented by Eq. (12). This potential range also causes Pd oxidation, as depicted in Eqs. (13) and (14), which may partly overlap with the dehydrogenation phase of the catalyst surface.

$$Pd + OH^- Pd \rightarrow OH_{ads} + e^- \quad (12)$$

$$Pd - OH_{ads} + OH^- \rightarrow Pd - O + H_2O + e^- \quad (13)$$

$$Pd - OH_{ads} + Pd - OH_{ads} \rightarrow Pd - O + H_2O \quad (14)$$

At a potential difference higher than 0.5 V vs. Ag/AgCl, the first step of oxide formation on the metal catalyst surface is the formation of a Pd(II) oxide layer. As the potential increases, the catalyst generates more metal oxides during the reverse scan condition, where the potential difference was between −0.25 and −1.20 V vs. Ag/AgCl. This is represented by Eq. (15) for Pd(II) oxide formation.

$$Pd - O + H_2O + 2e^- \rightarrow Pd - 2OH^- \quad (15)$$

The $PdCeO_2$/C catalyst was tested in a 0.1 M KOH solution doped with sorbitol at concentrations of 0.1 - 0.5 M, using a scan rate of 0.01 V/s. The oxidation reaction of the $PdCeO_2$/C catalyst was affected by the sorbitol solution doping. As an anode-side catalyst in an electrochemical cell, the $PdCeO_2$/C catalyst requires oxidation. The experiments showed that the $PdCeO_2$/C catalyst underwent oxidation in a potential range of −0.5 V to 0.5 V. At a concentration of 0.1 M KOH solution, the $PdCeO_2$/C catalyst exhibited a maximum oxidation current density of 0.2 mA/cm². The reduction activity of the catalyst decreased when increased with sorbitol and remained constant between concentrations of 0.3 to 0.5 M.

Performance of $PdCeO_2$/C vs. AgV_2O_5/C and $PdCeO_2$/C vs. $AgMnO_2$/C in sorbitol membraneless alkaline fuel cell

The fuel cell performances of the sorbitol membraneless alkaline fuel cell in this study are comparable to those of different cathode electrocatalyst. From performance test, results show that power density of $PdCeO_2$/C anode AgV_2O_5/C cathode (**Figure 13(B)**) are higher compared to $PdCeO_2$/C anode $AgMnO_2$/C cathode electrocatalysts (**Figure 13(A)**). The AgV_2O_5/C catalyst is an oxygen reduction reaction (ORR) catalyst which a trend of improvement in alkaline electrolyte solutions. As per the study, when the concentration of the sorbitol solution was increased, it is plausible that the oxidation of the alcohol functional groups was more effectively hindered.

The assessment of catalytic reduction reactions clearly demonstrated the glycerol tolerance exhibited by both the Ag/C and AgVxOy/C catalysts, as there were no observable oxidation reactions [11]. Based on this information, it can be inferred that the cathode catalyst, AgV_2O_5/C, possesses the capability to withstand the oxidation reaction of sorbitol. In terms of the anode catalyst, electrochemical evaluations revealed the remarkable catalytic efficiency and stability of the PdCeOx/C catalyst. This improvement can be attributed to several factors, including a larger electrochemically active surface area (ESA), electronic effects, and the presence of an increased quantity of oxygen-containing species facilitated by the CeOx [7]. Consequently, the fuel cell performance of the sorbitol membraneless alkaline fuel cell demonstrated higher power density for the $PdCeO_2$/C anode and AgV_2O_5/C cathode combination (**Figure 13(B)**).

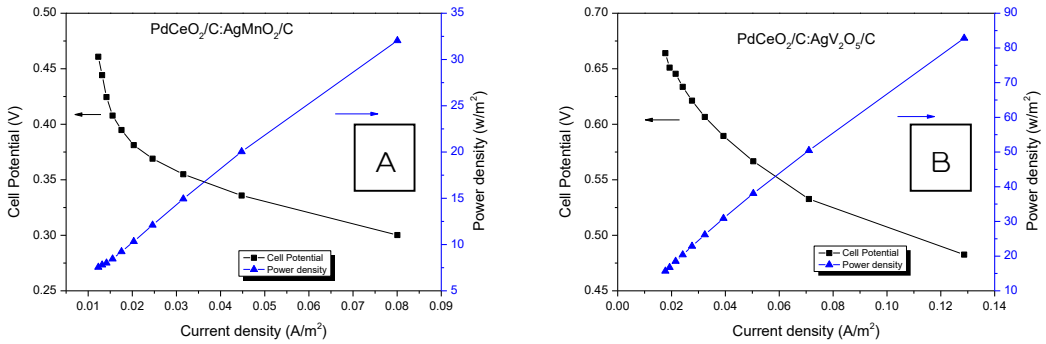

Figure 13 Polarization and power density curves for direct sorbitol fuel cell: (A) $PdCeO_2$/C anode $AgMnO_2$/C cathode and (B) $PdCeO_2$/C anode AgV_2O_5/C cathode.

Conclusions

In conclusion, the physical characterization of AgV_2O_5/C, $AgMnO_2$/C, and $PdCeO_2$/C catalysts showed that the metal particles agglomerate in a disorderly manner due to differences in their preparation steps. Electrochemical analysis by cyclic voltammetry revealed that $PdCeO_2$/C is a promising catalyst for the anode side, reaching a maximum oxidation peak at −0.5 to 0.1 V versus Ag/AgCl and a peak current density of 0.3 mA/cm^2 in 0.1 M KOH solution that was diluted with 0.1 to 0.5 M sorbitol. These findings highlight the potential of the $PdCeO_2$/C catalyst in electrochemical reactions and its suitability for use in certain applications. However, the cathode side tests with AgV_2O_5/C and $AgMnO_2$/C showed that the reduction reaction increased upon with sorbitol; it was observed that sorbitol had an effect on the reduction, and the catalysts must be resistant to cathode oxidation to obtain the most efficient and suitable electric cell. The performance test showed that the power density of the $PdCeO_2$/C anode and AgV_2O_5/C cathode was higher than that of the $PdCeO_2$/C anode and $AgMnO_2$/C cathode electrocatalysts. Therefore, it is important to choose a catalyst that is stable and durable in the environment for testing.

Acknowledgements

This research was supported by Thailand Science Research and Innovation (TSRI), Thailand funded 2022.

Nomenclature

JCPDS: Joint Committee on Powder Diffraction Standards

References

[1] I Cruz-Reyes, B Trujillo-Navarrete, K García-Tapia, MI Salazar-Gastéluma, F Paraguay-Delgado and RM Félix-Navarro. Pd/MnO_2 as a bifunctional electrocatalyst for potential application in alkaline fuel cells. *Fuel* 2020; **279**, 118470.

[2] F Bidault and PH Middleton. 4.07 - Alkaline fuel cells: Theory and application. *Compr. Renew. Energ.* 2012; **4**, 179-201.

[3] K Suwanraksa, P Masjod and C Chaiburi. Bimetallic of Pd-CeOx/C electrocatalyst for electro-oxidation reaction of xylitol fuels in alkaline solutions. *KKU Sci. J.* 2021; **49**, 165-73.

[4] K Suwanraksa, P Masjod and C Chaiburi. Electrochemistry of silver/metal oxide-based catalysts on carbon support for cathode electrode of reducing sugar alkaline fuel cells. *Burapha Sci. J.* 2022; **27**, 1226-37.

[5] I Stosevski, J Krsti, J Miliki, B Sljuki, Z Kcarevic-Popovi, S Mentus and S Miljani. Radiolitically synthesized nano Ag/C catalysts for oxygen reduction and borohydride oxidation reactions in alkaline media, for potential applications in fuel cells. *Energy* 2016; **101**, 79-90.

[6] Q Wu, L Jiang, L Qi, L Yuan, E Wang and G Sun. Electrocatalytic activity and stability of Ag-MnO_x/C composites toward oxygen reduction reaction in alkaline solution. *Electrochim. Acta* 2014; **123**, 167-75.

[7] L Feng, J Yang, Y Hu, J Zhu, C Liu and W Xing. Electrocatalytic properties of $PdCeO_x$/C anodic catalyst for formic acid electrooxidation. *J. Hydrogen Energ.* 2012; **37**, 4812-8.

[8] LJ Torres-Pacheco, L Álvarez-Contreras, V Lair, M Cassir, J Ledesma-García, M Guerra-Balcázar and N Arjona. Electrocatalytic evaluation of sorbitol oxidation as a promising fuel in energy conversion using Au/C, Pd/C and Au–Pd/C synthesized through ionic liquids. *Fuel* 2019; **250**, 103-16.

[9] LJ Torres-Pacheco, A Osornio-Villa, NA Garcia-Gomez, A Olivas, R Valdez, M Guerra-Balcazar, L Alvarez-Contreras and N Arjona. Effect of AuM (M: Ag, Pt & Pd) bimetallic nanoparticles on the sorbitol electro-oxidation in alkaline medium. *Fuel* 2020; **274**, 117864.

[10] LJ Torres-Pacheco, AD Leon-Rodriguez, L Alvarez-Contreras, M Guerra-Balcazar and N Arjona. Sorbitol electro-oxidation reaction on sub < 10 nm PtAu bimetallic nanoparticles. *Electrochim. Acta* 2020; **353**, 136593.

[11] C Chaiburi and R Jantong. Investigation of performance of glycerol-tolerant catalysts for cathodes of alkaline glycerol fuel cells. *KMUTT Res. Dev. J.* 2021; **44**, 443-55.

[12] Y Lu, Y Wang and W Chen. Silver nanorods for oxygen reduction: Strong effects of protecting ligand on the electrocatalytic activity. *J. Power Sourc.* 2011; **196**, 3033-8.
[13] MA Kostowskyj, D Kirk and S Thorpe. Ag and Ag–Mn nanowire catalysts for alkaline fuel cells. *Int. J. Hydrogen Energ.* 2010; **35**, 5666-72.
[14] S Ayyaru, S Mahalingam and YH Ahn. A non-noble V_2O_5 nanorods as an alternative cathode catalyst for microbial fuel cell applications. *Int. J. Hydrogen Energ.* 2019; **44**, 4974-84.
[15] D Basu and S Basu. A study on direct glucose and fructose alkaline fuel cell. *Electrochim. Acta* 2010; **55**, 5775-9.
[16] T Priamushko, R Guillet-Nicolas and F Kleitz. Mesoporous nanocast electrocatalysts for oxygen reduction and oxygen evolution reactions. *Inorganics* 2019; **7**, 98.
[17] P Masjod, K Suwanraksa and C Chaiburi. Development of binary catalysts support for the electro-oxidation reaction enhancement of glycerol alkaline fuel cell. *Thaksin Univ. J.* 2020; **23**, 55-64.